Journal of Sound and Vibration (1998) **211**(3), 513–520

DAMPING MEASUREMENTS IN FIBER REINFORCED COMPOSITE ROTORS

K. Gupta and S. P. Singh
Indian Institute of Technology, Hauz Khas, New Delhi-110016, *India*

(*Received* 1 *January* 1996, *and in final form* 28 *July* 1997)

1. INTRODUCTION

The present day rotors have predominantly metallic shafts. However, because of the greater specific strength and stiffness of high performance fibre reinforced composite materials, compared to metals, an attempt has been made to replace a metallic shaft by a composite shaft in some specific applications. The major developments over the past 20 years have taken place in the aerospace (helicopter) [1] and automotive industry [2]. Early developments in composite shafting which operated in the sub-critical range were directed towards design requirements and overcoming the practical problems in their development. Two US patents [3, 4] indicate that these problems were resolved in the 1980's. Subsequently, to derive greater advantage in terms of reduction in weight, the possibility of their supercritical operation [5] has been explored, necessitating rotor dynamic studies. Analytical and experimental studies on rotor dynamic aspects of composite rotors are few and relatively recent with little emphasis on estimation of passive damping in these rotors. Several experimental investigations on composite shafts with widely varying configurations are reported [6] in the literature which deal primarily with demonstration of sub- and super-critical operations, balancing, imbalance response and estimation of critical speeds. Developments in dynamics of composite shafting/rotors are traced in a recent review paper [7].

For non-rotating case, modal testing [8] on two shafts with 45° and 60° fibre angles with and without the lumped mass is carried out. Results show a higher damping for the 60° fibre angle shaft and also for shafts with a mounted lumped disc mass. Irretier [9] measured modal damping values in a non-rotating composite shaft in an attempt to predict delamination. Damping measurements in rotating composite shafts do not seem to have been made in any of the published literature. In the present paper, experimental results of modal damping in the first mode of a composite rotor mounted in rolling element bearings are presented. This is an extension of the previous work [8] in which modal testing was performed on non-rotating composite shafts. Damping measurements have also been made on rotating shafts by rapping and obtaining the decay curve after filtering out the components other than that corresponding to the damped natural frequency. The primary objective is to evaluate the effect of speed of rotation on first mode modal damping in a composite rotor. Using the half power point method, the imbalance response plot is used to get an effective measure of the rotor system damping. Damping values so obtained are compared with the theoretically predicted values and with earlier experimental results on non-rotating composite shafts [8].

2. EXPERIMENTAL INVESTIGATIONS

Measurements of damping by modal testing in a stationary rotor and by a rap test in the rotating as well as in the non-rotating condition are discussed here. In the non-rotating condition, measurements are made on four rotor configurations i.e., 45° fibre angle with

0022–460X/98/130513 + 08 $25.00/0/sv971320

(S45M) and without (S45) lumped mass and 60° fibre angle with (S60M) and without (S60) the lumped mass. In the rotating condition, damping measurements are made only on S60M at various rotor speeds in the range from 1000–3200 r.p.m.

2.1. *Experimental setup*

A tubular composite shaft 1·01 m long, mean radius 52 mm, wall thickness 5 mm, having a 7·5 kg disc at midspan and supported in rolling element bearings through metallic end flanges is shown in Figure 1. Carbon fibres (Hercules 929-6h (6K)) and epoxy resin (Ciba Geigy LY-556 and HT-972) are used. Two shafts were made with $\pm 45^\circ$ and $\pm 60^\circ$ degree fibre angles. Eddy current probes were used for measuring shaft motion in vertical and horizontal directions. A similar probe mounted at the flange acted as key phasor. The rotor was driven by a variable speed motor through a belt drive. No external load is connected, so the torque transmission through the rotor shaft is negligible.

2.2. *Test procedure*

A rap test was conducted on the shafts with and without the lumped mass for the purpose of damping measurement of the rotor in the rotating as well as in the non-rotating condition. For the non-rotating case, an accelerometer was mounted on the shaft and the response was recorded directly through the charge amplifier on a storage oscilloscope. From the decay plot, the log decrement was obtained and the damping ratio was estimated. The shaft, while in rotation, was rapped with a rubber mallet and the resultant transient response was measured by the vertical eddy current probe. To obtain the decay plots, a band pass filter tuned to the first rotor critical speed of 2244 r.p.m. (37·4 Hz), was used. The signal corresponding to the first rotor critical speed was filtered and captured on the oscilloscope. The rotor critical speed was experimentally obtained and thus includes the effect of damping on critical speed. The system damping ratio was then evaluated from the decay plot. Figure 2 shows typical experimental decay plots for the non-rotating case and at rotor speeds of 1960 and 3200 r.p.m. The decay plot for the non-rotating case (Figure 2(a)) gives the damped natural frequency of 37·2 Hz (2232 c.p.m.) which matches with the rotor critical speed of 2244 r.p.m. obtained from the imbalance response plot. This is expected since the disk gyroscopics are negligible. While at 3200 r.p.m. (Figure 2(c)), the plot exhibits only one dominant frequency corresponding to the rotor critical speed, at 1960 r.p.m. (Figure 2(b)) beating is observed because of the close proximity between the rotor operating speed and the first rotor critical speed.

2.3. *Discussion of experimental results*

Evaluation of damping by the log decrement formula implies a viscous equivalent of actual system damping. Since the actual damping is not viscous, but is primarily due to shaft material and other minor effects like friction in bearings, end-flanges, mounted lumped mass etc., damping values obtained from decay plots in present experiments are amplitude dependent. Damping values for the non-rotating case by modal testing [8] and

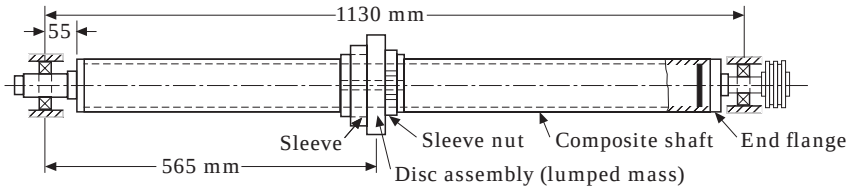

Figure 1. Test rotor for experiments.

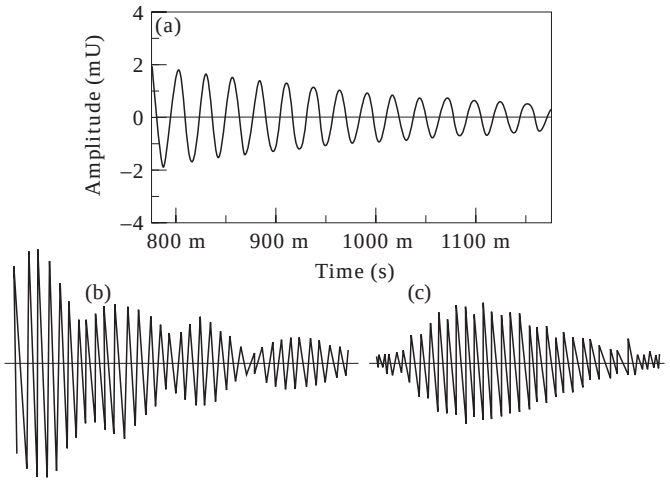

Figure 2. Experimental decay plots for S60M at (a) 0 r.p.m. (non-rotating case) (b) 1960 r.p.m. and (c) 3200 r.p.m.

by the rap test are given in Table 1. The variation of measured damping values for the S60M rotor with the operating speed varying in the range from 0–3200 r.p.m. is given in Table 2. At any constant rotational speed, some scatter in damping values obtained from cycle to cycle of a decay plot was observed. Average values are given in Table 2. Also, a problem is encountered when the decay plot shows beating as in Figure 2(b). The beating could be suppressed by using three percent bandwidth on the filter. However, complete elimination of beats could not be achieved when the rotor operating speed was close (within about 10%) to the rotor critical speed. At these speeds, the damping values are calculated such that both the included motions are in the same state of beat motion i.e., if the initial cycle is at the crest of beat, the final cycle should also be at the crest.

Damping values obtained from the rap test were found to be amplitude dependent. Analysis of decay plots revealed a larger damping ratio at higher displacement levels. Accordingly the range of damping values is given in row 2 of Table 1. Damping ratio by modal testing (row 1 of Table 1) will be an average value which, in all cases, falls in between

TABLE 1

First mode damping values (%) *by various methods*

	Rotor			
Method	S45	S45M	S60	S60M
Modal testing [8]	2·54	4·5	3·25	5·62
Rap test (non-rotating case)	1·6–3·0	1·6–3·3	–	1·7–6·2
Half power point method (rotating case)	–	1·42	–	2·26

TABLE 2

*Variation of modal damping with speed in S*60*M rotor*

Rotating speed (r.p.m.)	0	1000	1960	2460	3200
Damping (%)	1·7–6·2	1·0	0·9	1·3	1·6

the range of values indicated in row 2. Results of Table 1 show that, in all cases, system damping is higher for 60° fibre angle (S60 and S60M) shafts. This is explained by the more dominant contribution of the matrix, which has much higher damping compared to the fibres. Also, in experimental results of Table 1, shafts with lumped mass (S45M and S60M) show higher system damping compared to shafts without lumped mass (S45 and S60). This confirms the introduction of additional damping mechanism between the mounted lumped mass and the shaft. The two shafts with lumped masses were run beyond the first critical speed. From the imbalance response plots of these shafts shown in Figure 3, the damping ratio was obtained by the half power point method. These values given in the third row of Table 1 conform to the range of damping for both the shafts. However, it is to be noted that these values are representative of the shaft damping in the rotating condition. If damping is considered to vary with speed, then these values should be representative of the shaft damping in the vicinity of the critical speed.

Results of Table 2 show a definite decrease in system damping in the rotating condition. There appears to be a decreasing trend in damping with the rotor speed increasing up to about the first critical speed followed by a slight increase at speeds beyond the first critical. The experimental orbital analysis of the S60M rotor using vertical and horizontal eddy current probes revealed predominantly elliptical synchronous forward whirl orbits at all operating speeds other than the exact sub-harmonics (1/2, 1/3, 1/4 etc.) of the first critical speed of about 2244 r.p.m. Figure 4 shows the filtered compensated whirl orbits at 1003, 2145 and 2314 r.p.m. The orbit is highly elliptical at 1003 r.p.m. At 2149 r.p.m. also, it is elliptical, but the difference in the ellipse minor and major axis is relatively small compared to the lower speed of 1003 r.p.m. The whirl orbit is close to circular at 2314 r.p.m. The reduction in system damping in the rotating condition can be explained by the elliptical whirl orbit of the rotating shaft, as shown in Figure 5. If a non-rotating (zero speed)

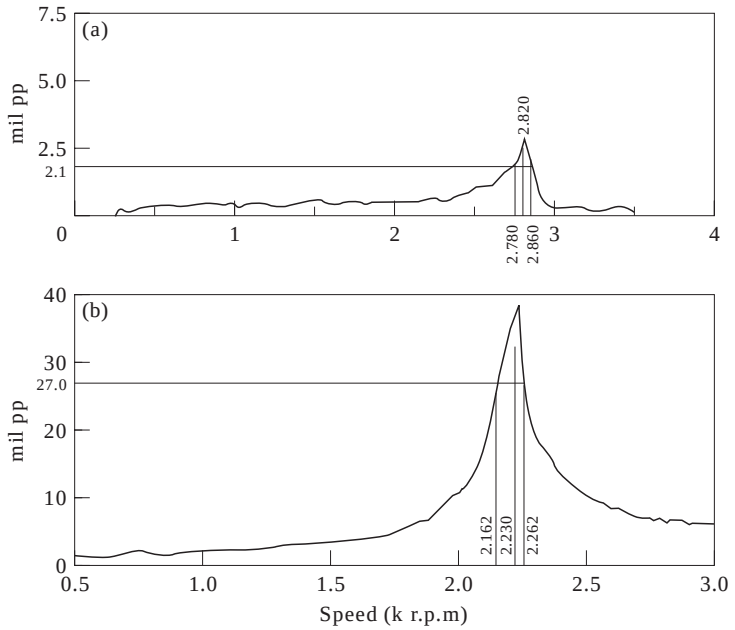

Figure 3. Imbalance response plots for (a) S45M and (b) S60M.

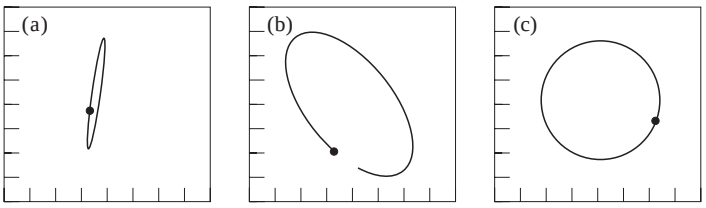

Figure 4. Compensated synchronous forward whirl orbits of S60M (rotation CCW) at (a) 1003 r.p.m., scale 2 mil/div; (b) 2145 r.p.m., scale 4 mil/div; and (c) 2314 r.p.m., scale 4 mil/div.

shaft/beam oscillates between two limits, it will experience completely reversed stresses and the energy dissipation in the shaft/beam due to material hysteresis effect will be maximum. For the shaft whirling in an elliptical orbit, the magnitude of the alternating component of the stress would be proportional to the difference of the magnitudes of the major and the minor axes of the ellipse. Thus for a shaft executing a synchronous forward elliptical whirl, as in the present case, the hysteresis effect and consequent system damping will be relatively smaller, compared to the non-rotating case in which the stresses will be completely reversed. It may be noted that if the shaft executes a forward synchronous circular whirl i.e., the major and minor axes become equal, then system damping will be practically nil. In rap tests, on the rotating shaft, two damping mechanisms are prevalent. The first is the up and down motion of the shaft, since it is impacted in the vertical direction. Superimposed on this is the second, the whirl motion of the shaft which is highly elliptical at low speeds. As explained already, the hysteresis effect will be present in both cases. However, in the first case i.e., the up and down motion is independent of rotational speed but is dependent on the intensity of the impact. The hysteresis effect, because of the second mechanism i.e., the nature of whirl orbit, is dependent on the rotational speed since the shape of the orbit itself is dependent on the rotor speed. It appears that the reduction in damping ratio with increasing speed is partly due to the second effect, as the whirl orbit is close to circular at speeds near the rotor critical (Figure 4). However, the fact that two mechanisms are present simultaneously and that the frequencies associated with the two motions are different i.e., the rotor natural frequency of about 2240 c.p.m. for up and down motion and the rotor operating speed for the whirl motion, causes the two motions to interact with each other resulting in an extremely complex picture as regards the shaft hysteresis.

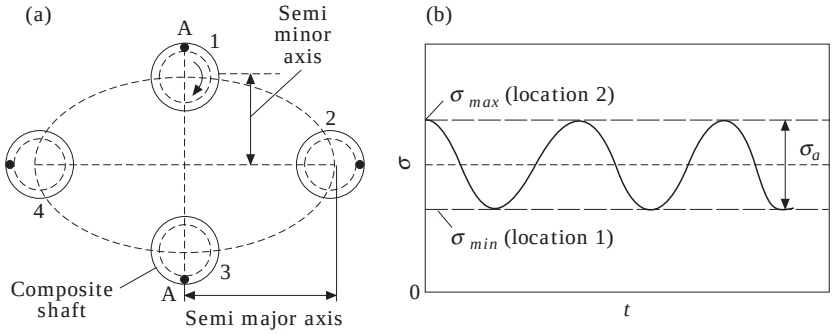

Figure 5. (a) An elliptical forward synchronous whirl and (b) variation of stress at point 'A' on shaft cross-section.

3. THEORETICAL ANALYSIS

The dynamic modelling of a composite rotor mounted on general, eight coefficient bearings by the energy method using Rayleigh–Ritz displacements is reported in detail in reference [10]. The strain energy of the shaft due to flexure in both the transverse planes and accounting for shear deformation effect is formulated. The kinetic energy of the shaft distibuted mass and a number of lumped disc masses due to translatory and rotary inertia effects is also formulated. The virtual work done by the bearing forces taking into account the bearing stiffness and damping coefficients, material damping and variation of energy associated with gyroscopic moments is formulated separately. A Rayleigh–Ritz displacement field in series form with unknown coefficients satisfying all geometric and complementary boundary conditions is assumed. By taking variations of rotor strain and kinetic energies with respect to solution coefficients and combining them with the virtual work due to bearing forces, material damping and gyroscopic moments, a complex quadratic eigenvalue problem is set up whose solution gives the rotor natural frequencies and the system damping. The above outlined energy approach is used for formulation of a rotor dynamic problem and evaluation of damping in the present case.

The properties of the experimental test rotor of section 2 are as reported in reference [11]. The loss factor for carbon fiber is taken as 0·0015 (0·15%) and that for the epoxy as 0·02 (2%). These are realistic values of loss factors for the carbon fibers and the epoxy which are well documented in literature, for example by Vantomme [12]. The values of the various moduli E_{11}, E_{22}, G_{12} and the corresponding loss factors η_{11}, η_{22} and η_{12} calculated from the well established relations based on micromechanics are as given below along with other rotor data; the volume fractions of fiber and epoxy were evaluated as 0·42 and 0·52 respectively, with 0·06 as void volume fraction: carbon/epoxy density = 1500 kg/m; $v_{12} = 0{\cdot}25$; $E_{11} = 117{\cdot}3$ GPa; $E_{22} = 7{\cdot}06$ GPa; $G_{12} = 3{\cdot}235$ GPa; $\eta_{11} = 0{\cdot}00179$; $\eta_{22} = 0{\cdot}0169$; $\eta_{12} = 0{\cdot}0196$; mass = 7·5 kg at midspan; lateral inertia of the mass = 0·013 kgm^2; polar mass moment of inertia = 0·026 kgm^2; length (L) = 1·01 m; radius = 0·052 m; thickness $t = 5$ mm comprising four layers.

For the purpose of comparison of measured damping values, the described theoretical formulation is used. The shaft mounted in rolling element bearings is assumed to be simply supported. The theoretical values of the damping ratio for various rotors are given in Table 3. The representation of material damping by the complex modulus is known to be approximate and has severe limitations when applied to a rotor problem. Since the complex modulus is not related to rotor whirl, it does not bring out the effect of rotational speed and the lumped mass on the system modal damping. Therefore, loss factor values given in Table 3 are independent of rotor speed. The internal damping in the rotors has two sources: (1) shaft material damping due to hysteresis effect and (2) dissipation of energy due to dry friction forces between mating components in assembled rotors. Conventionally, the internal damping force is taken to be proportional to the rate of the shaft deformation which, because of the shaft rotation effect, has a radial component which behaves in a manner similar to viscous damping and also has a destabilising speed dependent cross-radial component. Because of the destabilising cross radial component,

TABLE 3

Theoretical values of loss factor (%) *for different rotors*

Rotor	S45	S45M	S60	S60M
Loss factor	1·79	1·79	1·83	1·83

TABLE 4

Loss factor values (%) *for S*60*M with internal damping coefficient* ($H = 40{\cdot}3$ *Ns*/*m*)

Speed (r.p.m.)	0	500	1000	1500	2000	2200	2400
Loss factor (%)	*1·83*	1·45	1·08	0·68	0·35	0·15	0·0

the effective passive damping in the rotor is expected to decrease with increase in rotor speed. In the absence of any other passive damping, the cross radial component will render the rotor unstable at the first critical speed. This fact is illustrated in the results of Table 4, in which the loss factor for S60M rotor is evaluated at various operating speeds, taking the value of internal damping coefficient of $H = 40{\cdot}3$ Ns/m. Results shown in Table 4 indicate that the system loss factor value approaches zero as the operating speed approaches the rotor critical speed. In the present experiments, no instability of the rotor was observed at the first critical speed, which essentially means that some other dissipation mechanism, for example friction in rolling element bearings, was also present. However, it is clear that; in the present case, the destabilising cross radial component has partially contributed to the reduction in effective damping as the rotor speed increases (Table 2).

4. CONCLUSIONS AND FUTURE WORK DIRECTIONS

From the theoretical and experimental results of the paper, following conclusions can be made.

(1) The effective modal damping in the first mode seems to decrease with increase in operating speed up to the first rotor critical speed. This appears to be due to two reasons: (a) the shape of whirl orbit being highly elliptical at lower speeds and becoming almost circular near the critical speed and (b) the presence of a destabilising cross radial component of the shaft internal damping force.

(2) The modal damping ratio in the S60M rotor is approximately 1% (Table 2), which matches very well with the theoretical values of loss factor ($\eta = 2\xi$) of 1·83% (Table 3).

(3) The phenomenon of damping in the present case where the rotor is given an impact in the vertical direction is extremely complex because of simultaneous presence of up and down motion (due to impact) and the shaft whirl, both at their respective different frequencies.

Damping estimation in a rotating composite shaft needs to be substantiated by accurate theoretical modelling as well as elaborate experimentation. Work is being continued in the following directions. (1) Modal analysis of a rotating composite shafts needs to be undertaken and the results to be obtained should be compared to the present results. (2) Isolation of the different sources of damping *viz*., material, structural and external damping is necessary. (3) It is evident from the present experimental studies that damping values are dependent on the strain amplitude. The detailed quantitative study of this dependence is being investigated. (4) Theoretical rotordynamic modelling of a rotating composite shaft is necessary such that the available results for material in literature can be directly incorporated to get the system modal damping. (5) Damping behaviour of the shaft in the super critical range needs to be closely studied. (6) The damping analysis in rotors once established can be used to tailor the shaft material for optimized damping performance.

ACKNOWLEDGMENT

Support provided by the Aeronautics R&D Board in carrying out the above work is gratefully acknowledged.

REFERENCES

1. H. Zinberg and M. F. Symmonds 1970 *Presented at the* 26*th Annual National Forum of American Helicopter Society*, *Washington*, *D.C.*, *June* 1970. The development of an advanced composite tail rotor driveshaft.
2. H. S. Kliger and D. N. Yates 1980 *Advances in Composite Materials*, *ICCM*3, edited by A. R. Bunsell. Oxford: Pergamon Press. Design and material implications of composite drive shafts.
3. G. Worgan and D. Smith 1978 *US Patent* 4089190. Carbon fibre driveshaft.
4. D. Yates and D Smith 1979 *US Patent* 417626. Carbon fibre reinforced driveshafts.
5. J. W. Lim and M. S. Darlow 1986 *Journal of American Helicopter Society* **31**, 75–83. Optimal sizing of composite power transmission shafting.
6. K. Gupta and S. P. Singh 1996 *Indo-US Symposium on Emerging Trends in Vibration and Noise Engineering*, *IIT New Delhi*, 59–70. Dynamics of composite rotors.
7. S. P. Singh, H. B. H. Gubran and K. Gupta 1997 *International Journal of Rotating Machinery* **3**, 189–198. Developments in dynamics of composite material shafts.
8. S. P. Singh and K. Gupta 1993 *International Modal Analysis Conference*, *Florida*, *USA*, 733–739. Modal testing of tubular composite shafts.
9. H. Irretier 1993 DE- **64**, *Vibration*, *Shock*, *Damage and Identification of Mechanical Systems*, *ASME*, 23–38, Crack detection in composite driving shafts by experimental modal analysis.
10. S. P. Singh and K. Gupta 1996 *Journal of Sound and Vibration* **191**, 739–756. Composite shaft rotordynamic analysis using layerwise theory.
11. S. P. Singh and K. Gupta 1995 *Proceedings of the International Conference on Advances in Mechanical Engineering*, *Bangalore*, *India*, 1205–1221. Experimental studies on composite shafts.
12. J. Vantomme 1995 *Composites* **26**, 147–153. A parametric study of material damping in fibre-reinforced plastics.